International Journal of Sciences: Basic and Applied Research (IJSBAR)

ISSN 2307-4531
(Print & Online)

http://gssrr.org/index.php?journal=JournalOfBasicAndApplied

Bounds for the Propagation Model of Crack Forman

Cláudio Roberto Ávila da Silva Júnior [a]*, Rodrigo Villaca Santos [b]

[a] *NuMAT/PPGEM, Federal Technological University of Parana, Av. Sete de Setembro, 3165, Curitiba, 80230-901,Brazil*

[b] *DAMEC, Federal Technological University of Parana, Via do Conhecimento, Km 1, Pato Branco, 85503-390, Brazil*

[a]*Email: avila@utfpr.edu.br*

[b]*Email: rodrigov@utfpr.edu.br*

Abstract

Linear Elastic Fracture Mechanics (LEFM) describes the propagation of a crack exists in a material, and this propagation is proportional to the range of stress intensity factor. In LEFM there are several models that describe the evolution of an initial crack, as the models of Paris-Erdogan and Forman that are formulated and solved by the determination of an Initial Value Problem (IVP). For few practical applications, it is possible to obtain an exact solution of the IVP, and in most applications; approximate numerical solutions are used, which can reflect on aspects such as the time and the computational cost. Therefore, this paper presents a theoretical result establishing upper and lower bounds for the crack size function for Forman model. The bounds are very narrow, hence accurate crack size approximations can be obtained from only two stress intensity factor evaluations. This leads to a huge gain in a computational effort for numerical crack growth computations. Two examples are used within to explore the accuracy and efficiency of the proposed solution for the crack growth initial value problem.

Keywords: Crack; Forman; Initial Value Problem; Linear Elastic Fracture Mechanics

---

* Corresponding author.

E-mail address: avila@utfpr.edu.br.

1. Introduction

In linear elastic fracture mechanics, the rate of crack propagation $\left(da/dN\right)$ is assumed proportional to the range of stress intensity factors, (ΔK). In figure 1, Region I represents near-threshold crack growth. Region II represents intermediate crack propagation, where crack propagation rate is linearly proportional to ΔK (on a log-log scale) and where a small plastic zone appears ahead of the crack tip. Region II is the range of application of linear elastic fracture mechanics. Finally, Region III accounts for the accelerated crack growth just prior to failure. Non-linear fracture mechanics concepts are required to model crack growth in this region, as Forman model [1]. The Paris-Erdogan [2] crack propagation equation describes crack growth in the linear region (Region II in figure 1).

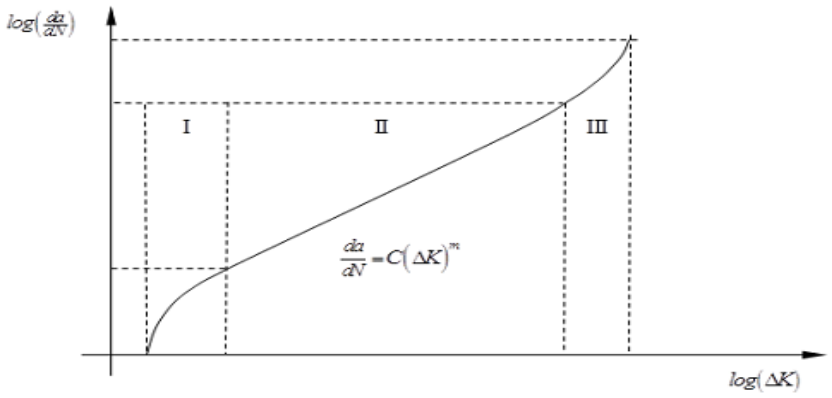

Figure 1: Diagram $log\left(\frac{da}{dN}\right) \times log\left(\Delta K\right)$.

Since only two parameters need to be identified, the Paris equation is widely employed in many applications. However, this equation is also known to present some major limitations: a. it only represents crack growth in region II (linear); b. mean stress effects are not taken into account and c. it neglects loading history and resulting load interaction effects. Several variants of the Paris equation have been developed to address these particular aspects. The model of Elber [3] uses an equivalent stress intensity factor to take into account crack closure under compressive stresses. The model of Forman includes mean stress and stress ratio effects. Many other models are available in the literature. Some of these models have found niche application; but none of them is overwhelmingly better than the others.

In order to simulate crack growth in components or structures with complex geometry, numerical analysis has been used extensively in recent years. This includes computation of stress intensity factors by the Boundary Element Method [4-6], Generalized FE methods [7-9], and Extended Finite Element Method [10-13], including cohesive crack modeling. Numerical computation of stress intensity factors and complex re-meshing schemes add significantly to the "computational burden" of crack growth estimation. This is especially the case when random crack propagation and/or reliability analysis is considered [14-19]; as uncertainty propagation studies increase the computational effort significantly.

Considering the aforementioned computational burden, this paper presents a theoretical result, in the form of a theorem, which allows evaluating upper and lower bounds for crack growth based on only two evaluations of the stress intensity factor. In this study, only the Forman crack propagation equation is considered. The bounds derived herein are based on polynomial functions of the number of load cycles. The examples presented herein consider problems with analytical geometry functions, but results can be readily extended to more general problems where stress intensity factors are computed numerically.

The remainder of this article is organized as follows. The Forman crack propagation equation is presented in Section 2. The theorem providing the crack growth bounds and it's proof are presented in Section 3. In Section 4, two example problems are addressed. Concluding remarks are presented in Section 5.

2. Forman crack propagation equation

Using the Forman crack propagation model, the crack growth problem can be written as,

$$\begin{cases} \text{Find } a \in C^1\left(N_o, N_1\right), \text{such that:} \\ \left(\dfrac{da}{dN}\right)(N) = \dfrac{C\left(\Delta K\left(a(N)\right)\right)^m}{(1-R)K_c - \Delta K}, \forall N \in \left(N_o, N_1\right); \\ a\left(N_o\right) = a_o. \end{cases} \tag{1}$$

Where C and m are material constants and N represents number of load cycles. The term $\Delta K(\cdot)$ is the range of stress intensity factors, defined as,

$$\begin{aligned} \Delta K\left(a(N)\right) &= \left(K_{max} - K_{min}\right)\left(a(N)\right) \\ &= \sqrt{\pi a(N)}\, f\left(a(N)\right)\left(\sigma_{max} - \sigma_{min}\right) \\ &= \sqrt{\pi a(N)}\, f\left(a(N)\right)\Delta\sigma. \end{aligned} \tag{2}$$

In Eq. (2), $f(\cdot)$ is the geometry function and $\Delta\sigma$ is the far-field stress range. The problem stated in Eq. (1) is classified as an initial value problem (IVP). Replacing Eq. (2) in Eq. (1), one obtains,

$$\begin{cases} \text{Find } a \in C^1\left(N_o, N_1\right), \text{such that:} \\ \left(\dfrac{da}{dN}\right)(N) = \dfrac{C\left(\sqrt{\Pi a(N)}\, f\left(a(N)\right)\Delta\sigma\right)^m}{(1-R)K_c - \Delta K}, \forall N \in \left(N_o, N_1\right); \\ a\left(N_o\right) = a_o. \end{cases} \tag{3}$$

Equation (3) is an IVP, defined by an ordinary, first order, non-linear autonomous differential equation. More generally, Eq. (3) can be classified as a Cauchy problem, which consists in finding the trajectories which satisfy the IVP differential equation and the initial value, $\left(a\left(N_0\right) = a_0\right)$. The existence and uniqueness of the solution to

this Cauchy problem depend on certain regularity conditions [20] on the functions at the right of Eq. (3). Interval (N_0, N_1) corresponds to load cycle $(\Delta\sigma)$ numbers, which are within Region II and III in figure 1.

3. Lower and upper bounds for crack size function

Lower and upper bounds for the crack size function are determined in this section based on the following hypotheses about the loading and the geometric correction function:

$$\begin{aligned}
&\text{H1}: \Delta\sigma(N) = \Delta\sigma_0, \forall N \in [N_0, N_1];\\
&\text{H2}: \begin{cases} f \in C^1([a_0, a_1]; \mathbb{R}^+ \setminus \{0\}); \\ 0 < f(a_0) \le f(x) \le f(y), x \le y, \forall\, x, y \in [a_0, a_1]; \\ f'(a_0) \le f'(x) \le f'(y), x \le y, \forall\, x, y \in [a_0, a_1]; \end{cases} \qquad (4)\\
&\text{H3}: m \ge 1;
\end{aligned}$$

Where $a_0 = a(N_0)$ and $a_1 = a(N_1)$. Hypotheses (H1) assumes constant loading. Hypothesis (H2) states that the geometry function must be a monotonously non-decreasing function, and that its derivative must also be a monotonously non-decreasing function. These conditions are met for most common geometry functions, since they represent an intrinsic characteristic of the crack propagation problem. And the hypothesis (H3) sets the value for the constant model of the material. Hypotheses (H1), (H2) and (H3) form the basis for the following theorem, which defines upper and lower bounds for the crack size function.

Theorem: Let $f(\cdot)$ and $\Delta\sigma(\cdot)$ be functions which satisfy hypotheses (H1) and (H2), respectively, and $a^* \in [a_0, a_1]$, the following lower and upper bounds are valid:

$$\begin{cases}
a(N) - a_o \le \begin{cases} \dfrac{C_F(\Delta K(a_0))^{m_F}}{(1-R)K_c - \Delta K(a_0)} + \dfrac{1}{2}\left[\dfrac{C_F\left(\Delta K\left(a^*\right)\right)^{m_F}}{(1-R)K_c - \Delta K\left(a^*\right)}\right]^2 \left[m_F + \dfrac{1}{(1-R)\dfrac{K_c}{\Delta K\left(a^*\right)} - 1}\right] \\ x\left[\dfrac{1}{2a^*} + \left(\dfrac{f'}{f}\right)\left(a^*\right)\right](N - N_o) \end{cases} (N - N_o); \\
a(N) - a_o \ge \dfrac{C_F(\Delta K(a_0))^{m_F}}{(1-R)K_c - \Delta K(a_0)} \begin{cases} 1 + \dfrac{1}{2}\left[\dfrac{C_F(\Delta K(a_0))^{m_F}}{(1-R)K_c - \Delta K(a_0)}\right]\left[m_F + \dfrac{1}{(1-R)\dfrac{K_c}{\Delta K(a_0)} - 1}\right] \\ x\left[\dfrac{1}{2a_0} + \left(\dfrac{f'}{f}\right)(a_0)\right](N - N_o) \end{cases} (N - N_o);
\end{cases} \qquad (5)$$

$\forall N \in [N_o, N_1]$.

Proof: From hypothesis (H2) and a second-order Taylor expansion of crack size, around a_0, one obtains,

$$a(N) = a_0 + \left(\tfrac{da}{dN}(N_0)\right)(N - N_0) + \tfrac{1}{2}\left(\tfrac{d^2a}{dN^2}(\eta)\right)(N - N_0)^2, \text{ with } \eta \in [N_0, N]. \quad (6)$$

The second-order term is called Lagrange's rest. Naturally, and from hypothesis (H2), the following inequalities can be written:

$$a(s) \le a(t),\ s \le t \text{ with } s,t \in [N_0, N] \Rightarrow (a(s))^m \le (a(t))^m.$$

From hypothesis (H2) one obtains,

$$(f(s))^m \le (f(t))^m \Rightarrow \left(a^{\frac{1}{2}}.f\right)^m(s) \le \left(a^{\frac{1}{2}}.f\right)^m(t),\ s \le t \text{ with } s,t \in [N_0, N].$$

Hence, one concludes that,

$$(\Delta K)^m (a(s)) \le (\Delta K)^m (a(t)),$$

Now, since $C > 0$ one obtains,

$$\tfrac{da}{dN}(s) \le \tfrac{da}{dN}(t),\ s \le t \text{ with } s,t \in [N_0, N].$$

The second derivative of the crack size function is evaluated as,

$$\begin{aligned}\frac{d^2a}{dN^2}(a(N)) &= \frac{d}{dN}\left(\frac{da}{dN}(a(N))\right) = \frac{d}{da}\left(\frac{da}{dN}(a)\right)\frac{da}{dN}(a(N)) \\ &= \left[\frac{C\Delta K^m}{(1-R)Kc - \Delta K}\right]^2 \left[m + \frac{1}{\frac{(1-R)Kc}{\Delta K} - 1}\right]\left[\frac{1}{2a} + \frac{f'(a)}{f(a)}\right].\end{aligned} \quad (7)$$

Inserting Eq. (7) in Eq. (6), the Taylor-expanded crack size function becomes,

$$\begin{aligned}a(N) - a_o = &\left[\frac{C\Delta K(a_0)^m}{(1-R)Kc - \Delta K(a_0)}\right](N - N_o) \\ &+ \frac{1}{2}\left[\frac{C\Delta K(a(\eta))^m}{(1-R)Kc - \Delta K(a(\eta))}\right]^2 \left[m + \frac{1}{\frac{(1-R)Kc}{\Delta K(a(\eta))} - 1}\right] \\ &\text{x}\left[\frac{1}{2(a(\eta))} + \left(\frac{f'}{f}\right)(a(\eta))\right](N - N_o)^2, \text{ with} \eta \in [N_o, N].\end{aligned} \quad (8)$$

The lower and upper bounds are obtained from a reformulation of Lagrange's rest in Eq. (8). From the behavior

of the geometric correction function in hypothesis (H2), the following inequality is proposed,

$$\left[f'(a)\sqrt{\Pi a} + \frac{f(a)\sqrt{\Pi}}{2\sqrt{a}} \right] \le \left[\sqrt{\Pi a^*}\, f(a^*) \right] \left[\frac{1}{2a^*} + \left(\frac{f'}{f} \right)(a^*) \right], \forall\ a \in [a_0, a_1]. \quad (9)$$

Similarly,

$$\left[f'(a)\sqrt{\Pi a} + \frac{f(a)\sqrt{\Pi}}{2\sqrt{a}} \right] \ge \left[\sqrt{\Pi a_0}\, f(a_0) \right] \left[\frac{1}{2a_0} + \left(\frac{f'}{f} \right)(a_0) \right], \forall\ a \in [a_0, a_1]. \quad (10)$$

Replacing Eq. (9) in Eq. (7), one obtains the following estimate,

$$\frac{d^2a}{dN^2}(\eta) \le \left[\frac{C\Delta K(a^*)^m}{(1-R)Kc - \Delta K(a^*)} \right]^2 \left[m + \frac{1}{\frac{(1-R)Kc}{\Delta K(a^*)} - 1} \right] \left[\frac{1}{2a^*} + \frac{f'(a^*)}{f(a^*)} \right], \forall\ \eta \in [a_0, a_1]. \quad (11)$$

The function leading to the lower bound is obtained by inserting Eq. (10) in Eq. (7),

$$\frac{d^2a}{dN^2}(\eta) \ge \left[\frac{C\Delta K(a_0)^m}{(1-R)Kc - \Delta K(a_0)} \right]^2 \left[m + \frac{1}{\frac{(1-R)Kc}{\Delta K(a_0)} - 1} \right] \left[\frac{1}{2a_0} + \frac{f'(a_0)}{f(a_0)} \right], \forall\ \eta \in [a_0, a_1]. \quad (12)$$

Replacing Eqs. (11) and (12) in Eq. (8), one obtains the upper and lower bounds stated in the theorem. It is noted that the lower and upper bounds for crack size, stated in the theorem, depend only on the evaluation of the geometry function and its derivative at two points, a_0 and a^*. The value a^* is related to Lagrange's rest for a second order Taylor expansion. Obtaining the coefficients of Eq. (5) only requires the evaluation of $\{ f(a_0), f'(a_0), f(a^*), f'(a^*) \}$. Hence, the computational cost for evaluating the bounds proposed in this paper is a small fraction of the computational cost for the traditional, cycle-by-cycle integration of Eq. (1). Clearly, the computed bounds depend on a proper choice for the value a^*. It is proposed that traditional engineering insight be used to select this value. For instance, the critical stress intensity factor, (K_{IC}), could be used to obtain a^*. In the numerical examples presented herein, narrow bounds are obtained for a^*=1,3 a_0.

4. Numerical examples

In order to evaluate the accuracy of the upper and lower bounds proposed in this paper (Eq. 5), the IVP in Eq. (3) is solved for two example problems. Since the differential equation is autonomous, Eq. (3) is separable; hence the crack size for any number of cycles can be obtained by direct integration, starting at the initial value. Unfortunately, analytical integration is possible only for a limited number of problems, for which the geometry function is analytical. For practical problems, numerical computation of stress intensity factors and numerical

integration is often required. In the examples below, the classical fourth-order Runge-Kutta method (RK4) [22] is employed:

$$\begin{cases} \text{Find } a_{k+1} \in \text{¡}^{+}, \text{such that :} \\ a_{k+1} = a_k + \left(\frac{\Delta N}{6}\right).\left(K_1 + 2K_2 + 2K_3 + K_4\right), \forall k \in \{0,1,...,n\}; \\ K_1 = C\left(\Delta\sigma\sqrt{\pi a_k}\, f_k\right)^m; \\ K_2 = a_k + \left(\frac{\Delta N}{2}\right).K_1; \\ K_3 = a_k + \left(\frac{\Delta N}{2}\right).K_2; \\ K_4 = a_k + \left(\Delta N\right).K_3; \\ a_0 = a\left(N_0\right); \end{cases} \quad (13)$$

Where $a_k = a\left(N_k\right)$, $f_k = f\left(a_k\right)$ and $\Delta N = N_{k+1} - N_k, \forall k \in \{0,1,...,n\}$. The RK4 method has precision of fourth order, $\left(O\left(\Delta N^4\right)\right)$.

In both numerical examples are used the following parameters given in Eq. (14).

$$\begin{cases} C = 6.9 \cdot 10^{-9}\,[\text{m / cycle}]; \quad m = 2.9; \quad N_0 = 0; \quad N_1 = 9 \cdot 10^5\,[\text{cycles}]; \\ a_0 = 1[\text{mm}]; \quad \text{b} = 100[\text{mm}]; \quad \Delta\sigma = 70[\text{MPa}], \forall N \in \left[0, 9 \cdot 10^5\right]. \end{cases} \quad (14)$$

The lower and upper bound crack size functions are second-degree polynomials in the number of cycles (*N*), and are defined as follows:

$$\begin{cases} a_{LB}\left(N\right) = \alpha N^2 + \beta N + a_0; \\ a_{UB}\left(N\right) = \gamma N^2 + \beta N + a_0, \forall N \in \left[0, 9 \cdot 10^5\right]. \end{cases} \quad (15)$$

For the two examples, the coefficients of these polynomials are presented in Table 1, whose definitions are given in Eq. (5).

Table 1: Polynomial coefficients of Eq. (15) for the example problems

Example	γ	α	β
1	2,21257464064954e-16	1,33674738809357e-16	4,2816531510184e-10
2	4,30927438837268e-16	2,59892738020747e-16	5,97026915762707e-10

Since the upper and lower bounds proposed in Eq. (5) are approximations to the actual crack size function, it is important to measure their accuracy with respect to the actual crack growth function. The following relative deviation function is introduced to this purpose:

$$\varepsilon_{UB,LB}\left(N_k\right)=100.\left(\frac{a_{UB,LB}(N_k)-a_{RK4}(N_k)}{a_{RK4}(N_k)}\right)[\%],\ \forall N_k \in \left\{0,50,100,...,9\cdot10^5\right\}. \quad (16)$$

4.1. Example1: finite width plate with center crack

Figure 2 shows the geometrical configuration of the finite width center cracked plate considered in Example 1. The geometry function is given by [23]:

$$f\left(a(N)\right)=\sqrt{sec\left(\frac{\pi a(N)}{2b}\right)},\quad \forall N \in \left[0,9\cdot10^5\right]. \quad (17)$$

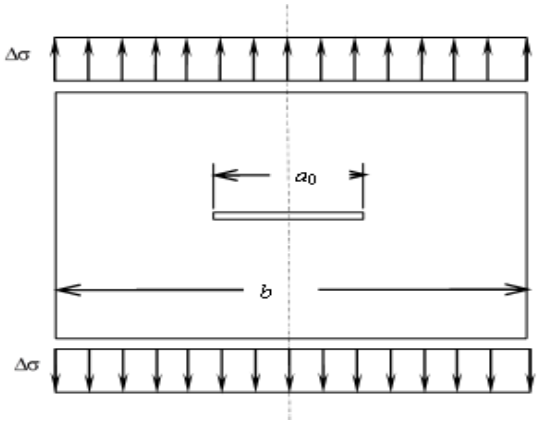

Figure 2: Finite width center-cracked plate, subject to tensile loading.

Results of crack size function, obtained by the RK4method, and the computed upper and lower bounds, are shown in figure 3. Figure 4 shows the relative deviation of upper and lower bounds in relation to the RK4method. In figures 3 and 4 one observes that the bounds proposed herein are quite narrow, providing accurate estimates of the actual crack size function.

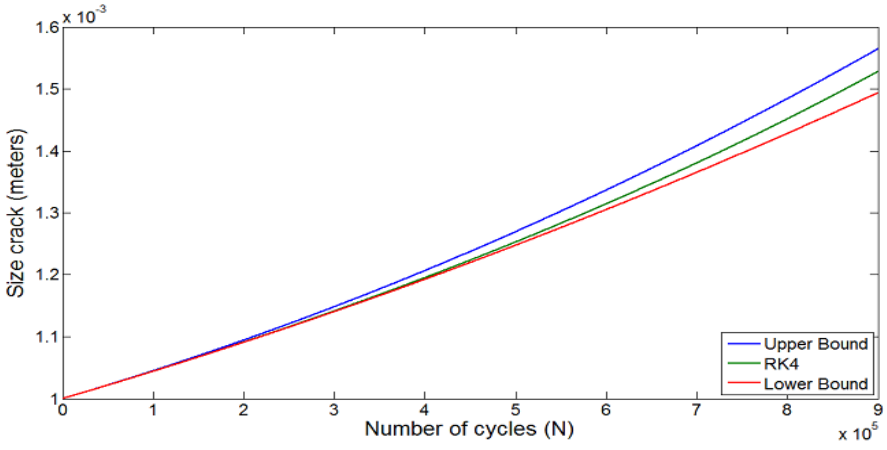

Figure 3: Crack size function and lower and upper bounds for example 1.

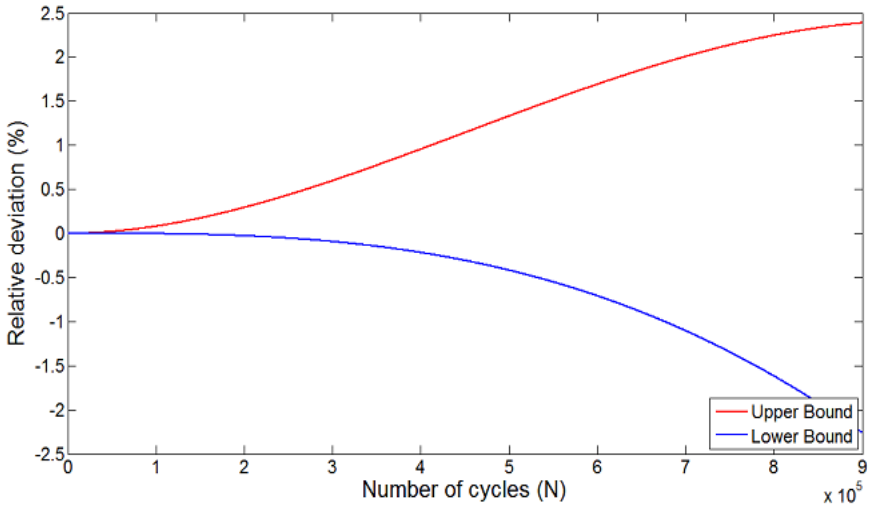

Figure 4: Relative deviation of lower and upper bounds for example 1.

4.2. Example 2: finite plate with a single edge crack

Figure 5 shows the geometrical configuration of the finite width plate with one edge crack considered in Example 2. The geometry function for this example is [23]:

$$f\left(a\left(N\right)\right)=1.122-0.231\left(\frac{a(N)}{b}\right)+10.55\left(\frac{a(N)}{b}\right)^{2} -21.72\left(\frac{a(N)}{b}\right)^{3}+30.39\left(\frac{a(N)}{b}\right)^{4},\forall N\in\left[0,9\cdot10^{5}\right]. \quad (18)$$

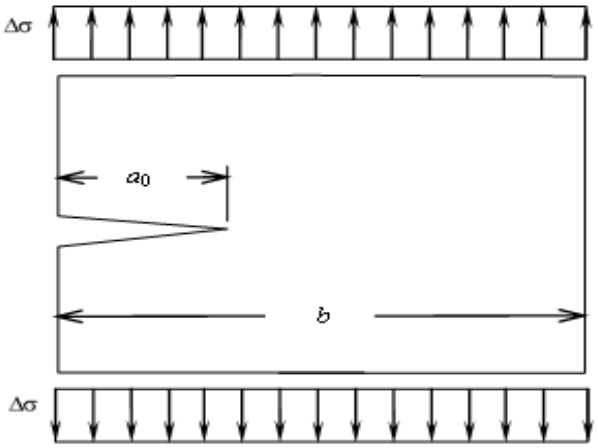

Figure 5: Finite width plate with one edge crack subject to tensile loading.

Figure 6 shows the numerical solution through the RK4 method for the crack size function, as well as the computed upper and lower bounds. Again, the bounds obtained with the proposed methodology are quite narrow, providing accurate estimates of the actual crack size.

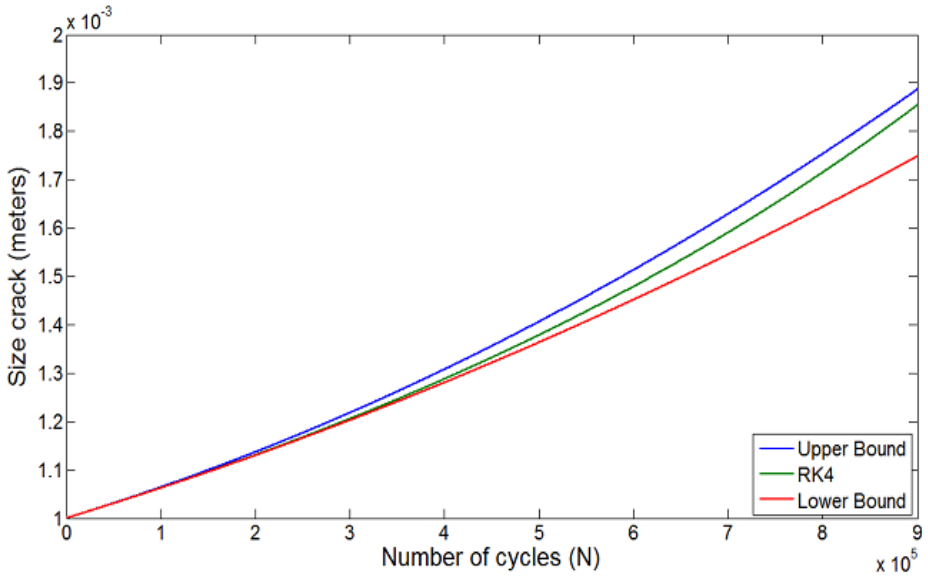

Figure 6: Crack size function and lower and upper bounds for example 2.

Figure 7 shows the relative deviation of upper and lower bounds in relation to the RK4method. A comparison of figures 4 and 7 reveals that, for this example, the relative deviation function for the lower bound, $(\varepsilon_{LB}(\cdot))$ assumed larger values. On the other hand, the relative deviation for the upper bound function was smaller and similar. For example 1, the largest deviation was $\varepsilon_{UB1} = 2.39\ \%$, and for example 2, the largest deviation was $\varepsilon_{UB2} = 2.42\ \%$.

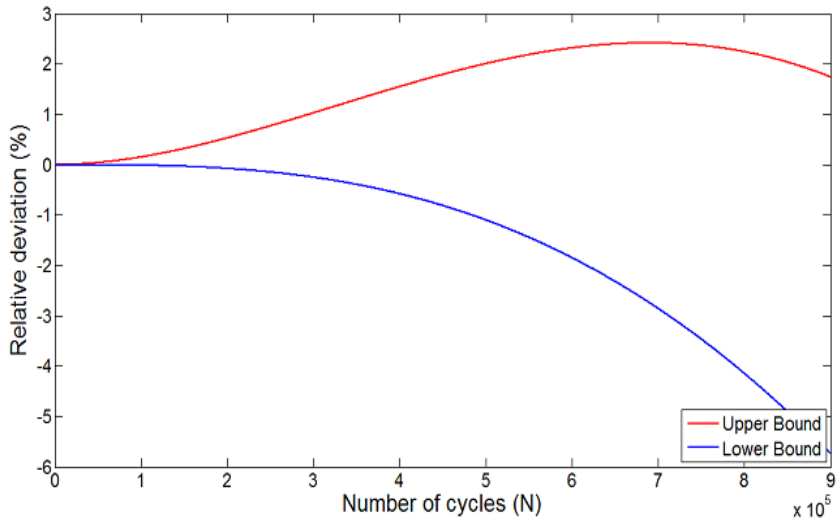

Figure 7: Relative deviation of lower and upper bounds for example 2.

4.3. Evaluation of the results

In both examples it is observed that the upper bound leads to smaller relative deviation. Table 2 shows the maximum and minimum values of relative deviation for the upper and lower bounds, $(max(\varepsilon_{UB}), min(\varepsilon_{LB}))$,

for both examples. In particular, it can be seen in Table 2 that the relative deviation with respect to lower bound, for example 2, resulted in larger value (in modulus).

Table 2: Maximum and minimum values of relative deviation $\left(max\left(\varepsilon_{UB}\right), min\left(\varepsilon_{LB}\right)\right)$, for upper and lower bounds, for examples 1 and 2

Example	$\max_k\left\{\left\{\varepsilon_{UB}\left(N_k\right)\right\}_{k=1}^{N_1}\right\},[\%]$	$\min_k\left\{\left\{\varepsilon_{LB}\left(N_k\right)\right\}_{k=1}^{N_1}\right\},[\%]$
1	2.39	-2.26
2	2.42	-5.73

Since computation of the bounds only requires evaluation of the geometry function (and it's derivative) for two crack sizes, it is much faster than direct numerical integration. For example 2, computing the bounds took only 0.0195 seconds, while numerical integration took 5.5767 seconds, leading to a reduction factor of 286 times. This result boosts the potential application of the bounds proposed herein to problems involving complex geometries and solution by numerical analysis.

The computed upper bound also depends, to some extent, on the choice of a^* points where geometry function and its derivative are evaluated. Figure 8 shows the upper bound, for example 2, with $a^*=1.2a_0,1.3a_0,1.5a_0$. It is observed that the upper bound functions are sensitive to different choices of a^*, since the coefficient "γ" in Eqs. (5) and (15) depends on a^*. It is proposed that engineering insight should be used to select a^*. The largest value of a^*, for instance, would be that leading to $f(a^*)=K_c$, where K_c is the critical stress intensity factor.

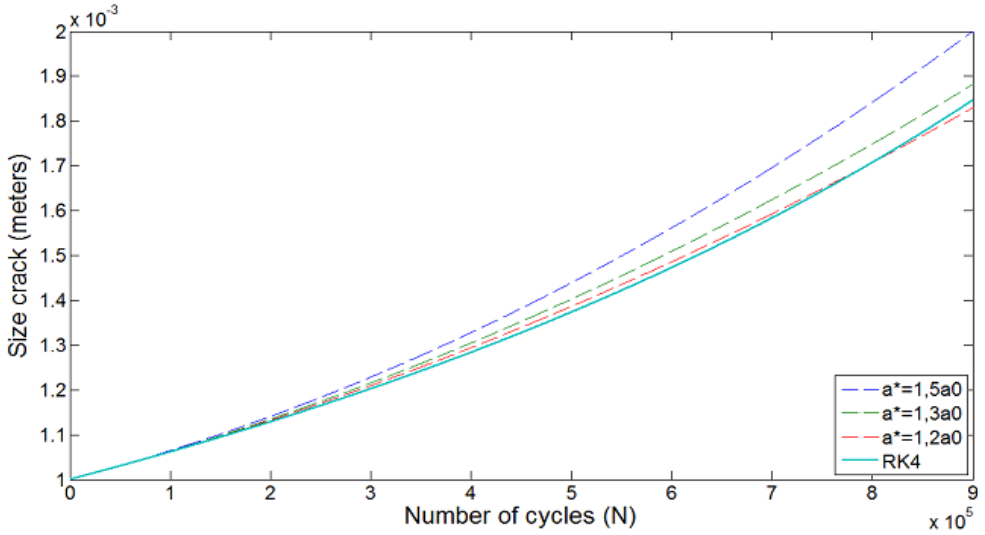

Figure 8: Crack size function and upper bounds (with $a^*=1.2a_0,1.3a_0,1.5a_0$) for example 2.

5. Conclusion

In this paper a classical result of calculus, the Lagrange's rest, was employed to propose a theorem providing lower and upper bounds for function crack size, based on the solution of an initial value problem involving the Forman model. The required assumption or hypothesis about the geometry function, i.e., that it be a monotonously non-decreasing function of crack size, is generally met in practice. Two polynomial functions are used to construct the lower and upper bounds. To evaluate the bounds one only needs to evaluate the geometry function and its derivative for two crack sizes. Hence, the reduction in computational effort is huge, when compared with direct numerical integration. This is especially true when the geometry function is not analytical, and stress intensity factors are evaluated numerically. The accuracy of the proposed bounds was evaluated for two example problems solved herein. In general, deviations were found to be around 2 to 6% for $a^* = 1.3a_0$, which can be acceptable for engineering purposes. This accuracy can be improved by a proper choice of the support point *a**. Results presented herein were based on a second order Taylor expansion, in order to avoid too many restrictions to be imposed on the geometry function. Considering a third-order Taylor expansion could lead to narrower bounds, but more restrictive hypotheses would be required on the geometry function.

References

[1] R. G. Forman, V. E. Kearney, R. M. Engle. "Numerical analysis of crack propagation in cyclic loaded structures." *J. Basic Engineering*, vol. 89, pp. 459-464, 1967.

[2] P. C. Paris, F. Erdogan. "A critical analysis of crack propagation laws." *J. Basic Eng.*, Trans. ASME. vol. 85, pp. 528-534, 1963.

[3] W. Elber. "Fatigue crack closure under cyclic tension." *Eng. Fract. Mech*, vol. 2, pp. 37–45, 1970.

[4] E. D. Leonel, W. S. Venturini. "Multiple random crack propagation using a boundary element formulation." *Engineering Fracture Mechanics*, vol. 78, pp. 1077-1090, 2011.

[5] E. D. Leonel, A. T. Beck, W. S. Venturini. "On the performance of response surface and direct coupling approaches in solution of random crack propagation problems." *Structural Safety*, vol. 33, pp. 261-274, 2011.

[6] E. D. Leonel, A. Chateauneuf, W. S. Venturini, P. Bressolette. "Coupled reliability and boundary element model for probabilistic fatigue life assessment in mixed mode crack propagation." *International Journal of Fatigue*, vol. 32, pp. 1823-1834, 2010.

[7] C. A. Duarte, O. N. Hamzeh, T. J. Liszka, W. W. Tworzydlo. "A generalized finite element method for the simulation of three-dimensional dynamic crack propagation." *Computer Methods in Applied Mechanics and Engineering*, vol. 190, pp. 15–17, 2227-2262, 2001.

[8] C. A. Duarte, D. J. Kim, D. M. Quaresma. "Arbitrarily smooth generalized finite element approximations." *Computer Methods in Applied Mechanics and Engineering*, vol. 196, pp. 1–3, 33-56, 2007.

[9] C. A. Duarte, D. J. Kim. "Analysis and applications of a generalized finite element method with global–local enrichment functions." *Computer Methods in Applied Mechanics and Engineering*, vol. 197, pp. 6–8, 487-504, 2008.

[10] J. Réthoré, S. Roux, F. Hild. "Mixed-mode crack propagation using a hybrid analytical and extended finite element method." *Comptes Rendus Mécanique*, vol. 338, pp. 121-126, 2010.

[11] Y. Shen, A. Lew. "Stability and convergence proofs for a discontinuous-Galerkin-based extended finite element method for fracture mechanics." *Computer Methods in Applied Mechanics and Engineering*, vol. 199, pp. 37–40, 2360-2382, 2010.

[12] T. Elguedj, A. Gravouil, A. Combescure. "Appropriate extended functions for X-FEM simulation of plastic fracture mechanics." *Computer Methods in Applied Mechanics and Engineering*, vol. 195, pp. 7–8, 501-515, 2006.

[13] P. Gupta, J. P. Pereira, D. J. Kim, C. A. Duarte, T. Eason. "Analysis of three-dimensional fracture mechanics problems: a non-intrusive approach using a generalized finite element method" *Engineering Fracture Mechanics*, vol. 90, pp. 41-64, 2012.

[14] D. A. Virkler, B. M. Hillberry, P. K. Goel. "The statistical nature of fatigue crack propagation." *Journal of Engineering Materials and Technology* (ASME), vol. 101, pp. 148-153, 1979.

[15] H. Ghonem, S. Dore. "Experimental study of the constant-probability crack growth curves under constant amplitude loading." *Engineering Fracture Mechanics*, vol. 27, pp. 1-25, 1987.

[16] J. W. Provan. *Probabilistic Fracture Mechanics and Reliability*, Dordrecht: Martinus Nijhoff, 1987.

[17] K. Sobczyk, B. F. Spencer. *Random Fatigue: From Data to Theory*, London: Academic Press, 1992.

[18] A. T. Beck, R. E. Melchers. "Overload failure of structural components under random crack propagation and loading - A Random Process Approach." *Structural Safety*, vol. 26, pp. 471-488, 2004.

[19] A. T. Beck, W. J. S. Gomes. "Stochastic fracture mechanics using polynomial chaos." *Probabilistic Engineering Mechanics*, vol. 34, pp. 26-39, 2013.

[20] E. A. Coddington. *An Introduction to Ordinary Differential Equations*, Dover, 1989.

[21] J. A. Ballantine, J. J. Conner, J. L. Handrock. *Fundamentals of Metal Fatigue Analysis*, New Jersey: Prentice Hall, 1989.

[22] U. M. Ascher, L. R. Petzold. *Computer methods for ordinary differential equations and differential-algebraic equations*. Philadelphia: SIAM, 1998.

[23] H. Tada, P. C. Paris, G. R. Irwin. *The stress analysis of crack handbook.* New York: ASME Press, 2000.